Assessment of Geriatric-Specific Changes in Brain Texture Complexity Using a Backpropagation Neural Network Classifier

R. Kalpana[*]
S. Muttan[†]
Department of Electronics and Communication Engineering
Anna University
Chennai 600025, India
[*]*kalpanatirth@gmail.com*
[†]*muthan_s@annauniv.edu*

A method to assess the aging of a human subject by modeling the devolution of the textural features in brain images using a backpropagation neural network (BPNN) is described in this paper. Normally, the brain white matter (BWM) undergoes degenerative changes in its physical and functional stochastics during the aging process. Relevant structural morphology observed in the brain complex can be measured via diffusion tensor magnetic resonance imaging (DTMRI). Using the underlying statistical details of the pixels in the brain image captured, BPNN is used to classify the distinct BWM parameters, which are then correlated to the subject's age. The brain complex invariably shows an evolutionary changing trend (in the negative direction) in its textural features during the aging process. Clinical DTMRI datasets from subjects of different age groups are used to study the efficacy of the proposed method of correlating brain-textural degeneration versus age.

1. Introduction

The brain textural format is a typical display of a biological pattern, which is "carefully crafted to satisfy some elaborate constraints" [1]. Ascertaining such brain textural characteristics is of clinical interest. Texture analysis can identify the underlying texture and express the patterns (associated with a smear of characteristic features) in quantitative terms.

The brain complex viewed for its stochastical features of macroscopic physical structure (anatomical aspects) and physio-neurological functions typically exemplifies a biological complex system as defined in [2]. Further, the brain complex invariably shows an evolutionary changing trend (in the negative direction) in its textural features during the aging process. Essentially, such changes indicate a decrease in myelin density as well as alterations in myelin structure [3]. That is, any morphology observed in the textural format of the brain complex manifests, for example, in the so-called cerebral white matter (also

https://doi.org/10.25088/ComplexSystems.20.4.305

known as brain white matter or BWM). Typically, such degenerative changes occur with the progress of normal aging and can be visually seen in the scanned images across the textural features. That is, geriatric-specific conditions introduce morphological artifacts to the image texture. Likewise, certain pathogenic symptoms may also indicate abnormalities in the regions of interconnecting white matter tracts [4].

Degenerative textural features in the BWM can be observed in the clinical images obtained via diffusion tensor magnetic resonance imaging (DTMRI) scans. By using such clinically scanned images of the brain, the associated textural features can be modeled, identified, and specified by a set of statistical parameters. Changes seen as distinct characteristics in the BWM (expressed via statistical measures) can be classified by a tool such as a backpropagation neural network (BPNN) trained to learn the mapping of such textural features.

The scope of this study includes: (*i*) obtaining clinical BWM images (via DTMRI scans) from adult subjects of different age subgroups (having no pathogenic conditions); (*ii*) estimating the textural complexity of the images in terms of statistical features; and (*iii*) using such statistical feature data as input vectors to train a BPNN, wherein data is mapped and stored as weight vectors with the output of the BPNN corresponding to each image depicting the age of the subject whose brain scan data is used. That is, the BPNN is designed to indicate the age linked to the image texture statistics; (*iv*) we exercise a prediction phase where the trained BPNN classifies a fresh set of brain image statistical features (addressed as input vectors) of a subject of unknown age by comparing the input data with trained vectors representing the patterns of the image and declare at the output the age of the subject.

In short, this study offers a BPNN-based method to classify a given brain image of a subject versus the age of the subject. That is, DTMRI images of the brains of human subjects (in the age group of about 50 to 80 years) are clinically collected and the specific feature data of BWM morphology is classified using a BPNN and correlated to the aging profile of the subjects.

2. Degenerative Features of the Brain versus Age of the Subject

BWM is a part of the brain made of cells called "axons" that connect massively to one another in a parallel architecture so that communication flows between neural cells. White matter gets its coloring due to the myelin coating of axon nerve fibers. Healthy aging is normally associated with morphological changes in the structure, physiology, and biochemistry of the brain. Brain size and weight inevitably decline with age. These changes begin in young adulthood but accelerate after the age of 60, resulting in about a 15% decrease in the ratio of

https://doi.org/10.25088/ComplexSystems.20.4.305

brain/skull volume [5]. Corresponding changes in BWM are commonly known as leukoaraiosis.

The textural features and associated changes in the BWM can be assessed via neuro-imaging [6, 7]. This technique allows scientific understanding of human brain development. Specifically, magnetic resonance imaging provides detailed images of brain anatomy with a clear definition of gray and white matter structures. The introduction of DTMRI offers a distinct way to observe such gray and white matter anatomy. This non-invasive three-dimensional modality measures the water molecule motion within the tissues using the magnetic resonance principle [8]. In this paper, DTMRI images obtained from the center of the corpus callosum of clinical subjects (adults) are used and analyzed in terms of their features characterized by statistical parameters. The scope of this study would lead to understanding the morphology of BWM versus age. Any abnormal changes observed that are inconsistent with the age would mean possible pathological conditions.

In this paper, relevant to the objective of correlating the scanned local image data of the BWM (having degenerative attributes) versus the age of the subject, an image classification method is pursued.

3. Analysis of Brain Textural Complexity

Recognizing specific textural features in an image is a well-known image processing technique [9]. Acquisition of such image feature information is in essence a pattern recognition process. It can be done by a system, which takes the set of pattern/feature details and identifies it as a specific class (among a number of previously known classes). Functionally, such pattern-recognition systems (or machines) need an input vector set depicting the characteristic features of the test image. It can then associate the input vector set as closely as possible to a known set of patterns (stored as key vectors) and declare an output vector specifying the class of the pattern consistent with the input information.

Relevant recognition of textural features in an image (e.g., of the brain) involves the following basic steps.

> Step 1: Modeling the textural features of the test image to yield the necessary input vector set for pattern analysis
>
> Step 2: Constructing an image-processing machine and exercising training phase of the machine to learn and store key patterns pertinent to a set of input vector patterns
>
> Step 3: Addressing the machine with a fresh input test pattern to be classified so that the machine performs an association of the input vector with the set of stored key patterns toward classification; hence, the machine declares the input test vector belonging to a specific class (of known feature characteristics)

https://doi.org/10.25088/ComplexSystems.20.4.305

Step 1 involves formulating the necessary input vector set of the underlying image textural features. For this purpose, the test image texture has to be modeled so as to yield necessary input vectors for use in the image-processing machine. For example, pertinent to textural aspects of brain complexity, a cellular automaton (CA) model has been indicated by S. Wolfram [1]. Essentially, a CA model is specified by the underlying dynamics of the system, mostly discrete in space, time, and state variables [10]. Further, a CA is considered as a good model for the study of nonlinear complex systems characterized by possession of exclusively local mechanisms of interaction. Inspired by this notion, Wolfram [1] advocates that "images can be specified notably with systems equivalent to additive cellular automata" and a CA is convenient in depicting distinctive features as in the brain complex.

Notwithstanding the elegance and feasibility of CA modeling toward textural analysis of images, there are also other avenues of image-analysis methods indicated in the literature [4, 9].

In the present study, relevant modeling of textural features in the brain complex toward image classification is done via statistical characterization of the image structure. That is, textural features of images are elucidated in terms of statistical norms on the basis of gray-tone spatial dependencies toward image classification. The heuristics of this approach are as follows. Textural features possess information about the spatial distribution of tonal variations within a band. Such spatial dependence of feature statistics across the image pixels can be gathered as parameters for use as input vectors in an image-classification machine.

4. Statistical Characterization of Image-Textural Features: Gray Level Cooccurrence Matrix Approach

Gray levels of a two-dimensional (2D) image can be formalized in terms of the gray level cooccurrence matrix (GLCM). The basics of the GLCM approach are as follows.

For each test image (such as the brain scan obtained via clinical DTMRI), a 2D histogram of gray levels distinguishing a pair of pixels (separated by a fixed spatial relationship) can be constructed. A relevant matrix denotes the GLCM of the test image. It is sized to accommodate the number of gray levels with the cooccurrence probabilities stored as the elements of the matrix. Thus, GLCM quantitatively describes the associated gray level statistical variations in the image. It is therefore expected that any statistical feature changes seen in the image (manifesting as gray-level changes across 2D pixels), as a result of aging or otherwise, should imply corresponding variations in the measured GLCM parameters. If such statistical attributes of gray-level changes are classified and extracted from the test image data, they can then be used as metrics toward correlating the observed morphology

https://doi.org/10.25088/ComplexSystems.20.4.305

to the aging process. The procedural aspect of constructing a GLCM is outlined below.

In image analysis, apart from size, shape, and color, texture is a property widely considered as an input vector. Texture can be defined as a function of the spatial variation in pixel intensities. Typically, repetition of some basic pattern is involved in texture attributes and as such, textural details provide information about the structural arrangement of surfaces. Such details get mapped into the images captured via scanning the surfaces of interest. The associated textural feature information can be extracted by texture analysis toward image coding.

An application of image-texture analysis, for example, is the recognition of specific image regions and classifying them in terms of the associated statistics of texture properties. In such image-texture analyses, for the purpose of classification, the complex test texture has to first be specified in terms of a certain number of measurable features or parameters (step 1). In the relevant procedures, statistical measures on the image section being analyzed can be defined and used.

If the GLCM concept is used in such pursuits, the textural characteristics can be identified and defined in terms of 13 texture features as proposed by Haralick et al. [11]. Relevant algorithms denote statistical measures of image texture features such as homogeneity, gray-tone linear dependency, contrast, number and nature of boundaries present, the complexity of the image, and more. Such Haralick parameters are determined from the GLCM based on cooccurrence probabilities.

In summary, given an image composed of pixels each with an intensity with a probabilistic value of gray level, the corresponding GLCM is a tabulation of how often different combinations of gray levels cooccur in an image or an image section. It estimates image properties via statistics aspects of the pixel details. Such image properties (commonly known as Haralick texture features) are used in this study for image classification [11]. That is, having constructed a GLCM depicting the image textural statistics of the test image, the associated local features can be sorted out by means of a classifying tool/machine.

For the purpose of constructing the GLCM of an image, a displacement vector $\mathbf{d}$ with reference to a pixel (expressed by a radial distance δ and orientation angle θ) is defined so as to decide on relative pixel-to-pixel locations and their extent of correlation. Every pixel is considered to have eight neighboring pixels allowing θ to be 0°, 45°, 90°, 135°, 180°, 225°, 270°, or 315°. However, considering the diagonal symmetry of the matrix format of the GLCM, the cooccurring pairs obtained by choosing θ equal to 0° are the same as θ being 180°. Likewise, this concept extends to 45°, 90°, and 135°, as well. Therefore, there are four choices in selecting the value of θ.

Pertinent to the choice of quantized gray levels, the dimension of a GLCM is determined by the maximum gray value of the pixel. The number of gray levels is an important factor in GLCM computation.

https://doi.org/10.25088/ComplexSystems.20.4.305

More levels would mean a more accurate depiction of textural information, but it implies more computational costs.

Figure 1 illustrates the plane (2D form) of the brain sliced and scanned in the experiment. Relevant pixel-by-pixel gray-level intensity measured across the 2D profile is denoted by $\vartheta(x_m, y_n)$ at any coordinate (x_m, y_n). The scale of intensity level is indicated by ℓ_{mn}. Also, the size of the GLCM is $(M \times N)$ with $m = 1, 2, \ldots, M$ and $n = 1, 2, \ldots, N$.

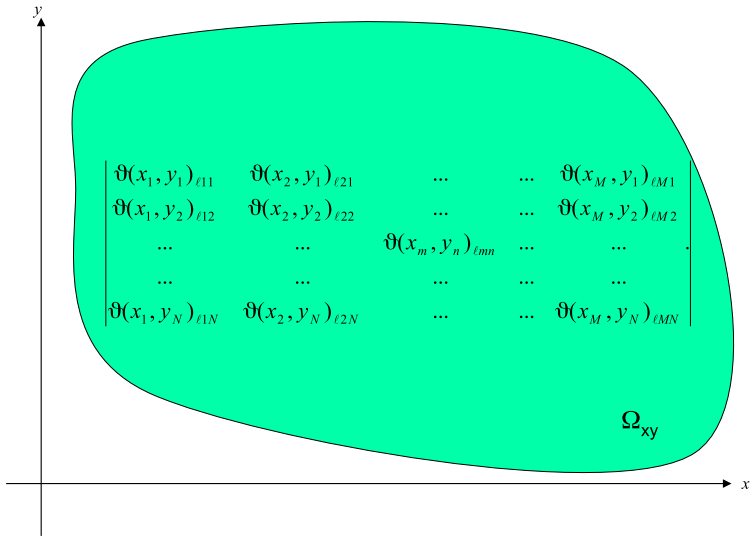

Figure 1. Universe of a 2D BWM surface with the associated intensities of gray levels along the x and y axes.

Consider two pixels at the coordinates $(x_a, y_b) \in \{x_m, y_n\}$ and $(x_c, y_d) \in \{x_m, y_n\}$ in the (x, y) space depicting the 2D brain structure of Figure 2. Let the measured gray-level intensities at these locations be $\vartheta(x_a, y_b)_{\ell_{ab}}$ and $\vartheta(x_c, y_d)_{\ell_{cd}}$, respectively. Further, $0 \le \ell_{\text{mn}} \le L$ denotes the scale of integer values of the gray level at (x_m, y_n), with zero representing the black level and L denoting the maximum gray level toward white). The Euclidean distance between (x_a, y_b) and (x_c, y_d) is denoted by a vector $\mathbf{d}_{\text{ab-cd}}$.

Using the ϑ matrix in the (x, y) plane, $\{\vartheta(x_m, y_n)_{\ell_{\text{mn}}}\}$ as illustrated in Figure 1, four other matrices can be constructed involving θ.

- *Horizontal* ($\theta = 0°$) *matrix* (H_o *matrix*): Consider any arbitrary element $\vartheta(x_m, y_n)_{\ell_{\text{mn}}}$ in the ϑ matrix and note its gray-scale (integer) value ℓ_{mn} lying in the range $0 \le \ell_{\text{mn}} \le L$. Scan the entire row (horizontal scan) containing this element and count the number of times the ℓ_{mn}

https://doi.org/10.25088/ComplexSystems.20.4.305

value cooccurs as the neighbor (implying $|\mathbf{d}| = 1$), 0, 1, … and L. The count value is denoted as h. This is repeated for each row starting with $\ell_{11}, \ell_{12}, \ldots, \ell_{1N}$. The resulting matrix is constructed as shown in Figure 2(a).

- *Vertical* ($\theta = 90°$) *matrix* (V_{90} *matrix*): Similar to the H_o matrix construction, scanning vertically along each column of the ϑ matrix, the resulting V_{90} matrix is obtained as illustrated in Figure 2(b), where v stands for the count of cooccurring values along the vertical direction and horizontal direction, respectively.
- *Slant* ($\theta = 45°$, $\theta = 135°$) *matrix* (s_{45}, s_{135} *matrix*): Likewise, a diagonal count matrix along the 45° slant and the 135° slant can be specified as shown in Figure 3, where s_{45} and s_{135} represent the count of cooccurring values diagonally along 45 and 135 degrees, respectively.

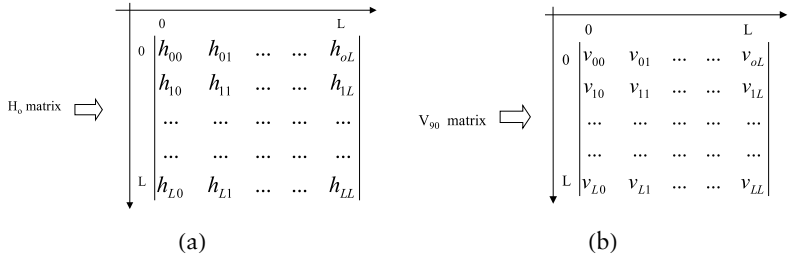

Figure 2. Matrix representation of (a) horizontal and (b) vertical cooccurrences of gray levels.

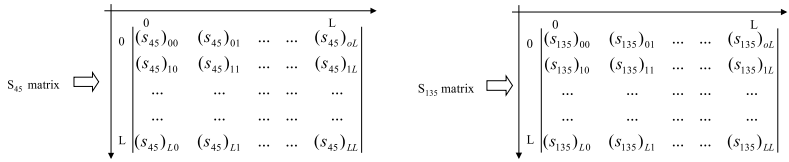

Figure 3. Matrix representing diagonal cooccurrences of gray levels.

The four matrices indicated earlier denote implicitly the intensity level count variations in terms of the gradient, and by determining such intensity variations along the four directions, account for the associated anisotropy of the image. Further, an average of the four cooccurrence matrices can be taken to ensure rotational invariance as suggested by Caban et al. [12]. However, in the present study, each of the four matrices is considered separately in order to evaluate the statistical feature map of the BWM under discussion on an ensemble basis; the statistical features evaluated for the four matrices are then averaged. This would again maintain the rotational invariance and the anisotropy considerations.

https://doi.org/10.25088/ComplexSystems.20.4.305

Now, the method of deducing GLCM-based statistical parameters can be considered. These parameters can be explicitly specified by the underlying statistics of the image data compiled. They can be grouped into the following categories of entities.

- *Energy*: This measures the textural uniformity of pixel pair repetitions, which is deduced via angular second moment of the statistics. High energy values imply the gray level distribution is constant or in periodic form. In the normalized format, the maximum level of computed energy is set equal to one. A less homogeneous image would present a large number of small entries in the GLCM.
- *Entropy*: This statistic measures the "disorder" of an image. Again, large entropy means the image is not texturally uniform. As such, several of the GLCM elements will have low values. Complex textures of random features will tend to have higher entropy. Entropy metric is an inverse of energy-specific metric.
- *Contrast*: The statistical attributes of an image expressed via spatial frequency signifies the contrast feature, which can be deduced by difference moment of the GLCM. It is the difference between the highest and the lowest values of a contiguous set of pixels and measures the amount of local variations present in the image. A low-contrast image presents a GLCM concentration term around the principal diagonal and features low spatial frequencies.
- *Variance*: This statistic measures heterogeneity and is related to the first-order statistical variable, namely standard deviation. Variance is the spread around the central tendency; therefore it increases with the gray level values differing (spreading) from their mean.
- *Homogeneity*: Known as inverse difference moment, the associated statistic measures the extent of homogeneity of the image in terms of larger values for smaller gray tone differences in pair elements. It is more sensitive to the presence of near-diagonal elements in the GLCM and has maximum value when all elements in the image are identical. The GLCM contrast metric is an inverse of the homogeneity measure when both are expressed in terms of an equivalent distribution of the pixel pairs population. It means homogeneity would decrease if contrast increases, keeping the energy level invariant.
- *Correlation*: The correlation feature is a measure of gray tone linear dependencies in the image.

Consistent with these notions of quantifying the image statistics, Haralick et al. [11] proposed 14 textural features that can be deduced via GLCM [13]. Explicitly, these refer to the following metrics: (1) angular second moment; (2) contrast; (3) correlation; (4) sum of squares variance; (5) inverse difference moment; (6) sum average; (7) sum variance; (8) sum entropy; (9) entropy; (10) difference variance; (11) difference entropy; (12–13) a pair of information measures of correlation (in Shannon's sense); and (14) maximal correlation coefficient. Relevant definitions and algorithms are explicitly furnished in [11]. However, only 13 features (1 to 13) are computed and used in this study.

https://doi.org/10.25088/ComplexSystems.20.4.305

5. Image Classification Based on Pixel-Feature Statistics

As summarized in Section 3, recognizing textural features in an image (e.g., of the brain) involves three basic steps: (*i*) modeling textural image features to get the necessary input parameter vector set for pattern analysis (step 1); (*ii*) creating an image-processing machine and training it to learn and store known key patterns (step 2); and (*iii*) addressing the details of any test pattern (to be classified) as the input parameter vector set to the machine, where an association of the input vector with the set of stored key patterns is done; hence, the input data is classified and declared as belonging to a specific class of known feature characteristics (step 3).

The texture classification of step 2 can be done in a classifier or image-processing machine. A variety of pattern classification algorithms to compare the input vector set with the stored key patterns has been indicated in the literature [9]. Popular methods include the artificial neural network (ANN) [14], genetic algorithm-based machines, maximum-likelihood classifier, minimum-distance classifier, statistical discrimination or information theoretic-based classifying machine, syntactic classifier, graph-theoretic matching machine, various machine-intelligence concepts, swarm intelligence approach (such as fish flocking or ant-colony schemes), and biologically inspired divergence-based classifiers.

In this study, the ANN adopted functions as a trainable classifier using a BPNN architecture. The training set (TS) corresponds to the input vectors gathered from test images of BWM obtained via clinical DTMRI scans. Those input feature vectors referred to an ensemble of the details acquired from the GLCM-based set of Haralick parameters (13 Haralick parameters obtained from each sample image and so from 60 DTMRI scanned images). Thus learning of the network corresponds to 60 ensemble runs of training executed, each with 13 feature values at the network input.

The network is trained (or made to learn) a test image by comparing its output with a supervising teacher value. In this context, the teacher value corresponds to the known age of the subject whose scanned brain image data forms the input vector set. Thus, using a number of images, the BPNN is trained with the TS of each image. These images used in the training phase are stored in the classifier as key vectors for future comparison with any new images intended for classification.

In the prediction phase, if a vector set description of a new BWM image is addressed at the input of the network, this image information will be classified (and correlated to the age of the subject) at the BPNN output. Thus, with the acquisition of clinical DTMRI data of BWM of any subject, the relevant dataset is preprocessed to capture its statistical features (through GLCM-based Haralick parameters) and addressed as the input to the trained BPNN, which will classify how the input belongs among the stored key patterns of feature

https://doi.org/10.25088/ComplexSystems.20.4.305

vectors. Hence, it will predict the age of the subject (as its output) versus the input BWM characteristics.

The computational steps of the BPNN training are indicated in Figure 4 and a similar pursuit is also exercised in the prediction phase. The description of the BPNN architecture used is described in Section 6.

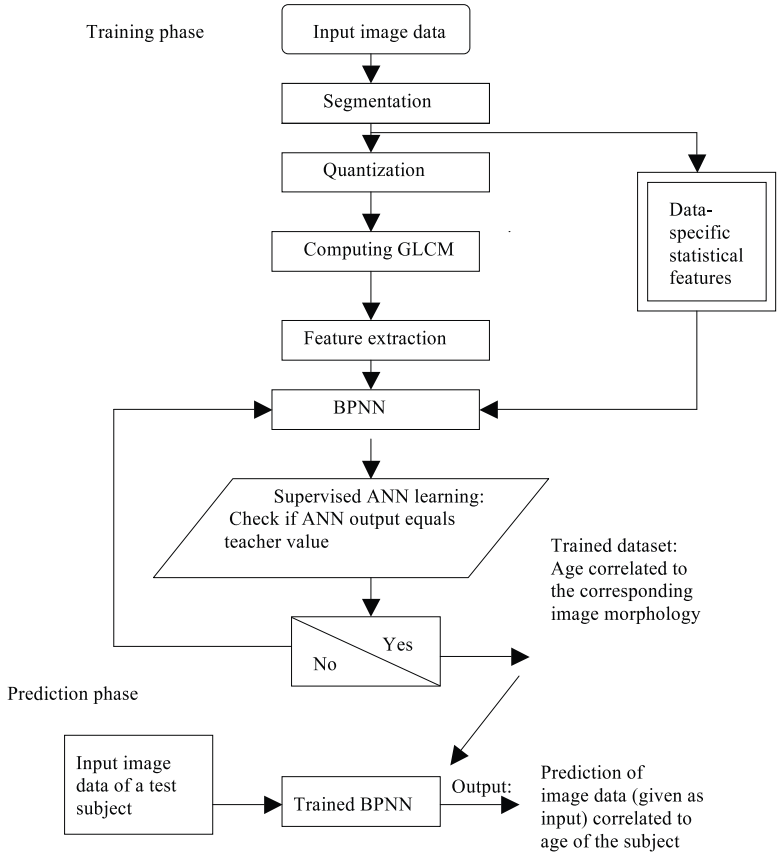

Figure 4. Flow chart depicting BPNN-based test procedure to correlate the changes measured in BWM versus aging.

6. Backpropagation Neural Network Classifier: Description

BPNN is a collective network of massively interconnected sets of neural units. One of the network's abilities is to enable the functionality of a classifier. In this paper, a BPNN architecture is adopted to classify the images as required. The BPNN is built with four input

https://doi.org/10.25088/ComplexSystems.20.4.305

neurons (to take a set of four input vectors) and can be expanded to accommodate 13 input vectors corresponding to the Haralick parameters when needed.

At the output formed by a single neuron, a teacher value (age of the brain image subject) is specified toward supervised learning as shown in Figure 5. Furthermore, this test network has two hidden layers, each with eight neurons. (Selection of the number of neurons in the hidden layer is done by trial and error. With a few neurons—four, for example—the network did not converge. Excess neurons increase the computational complexity.)

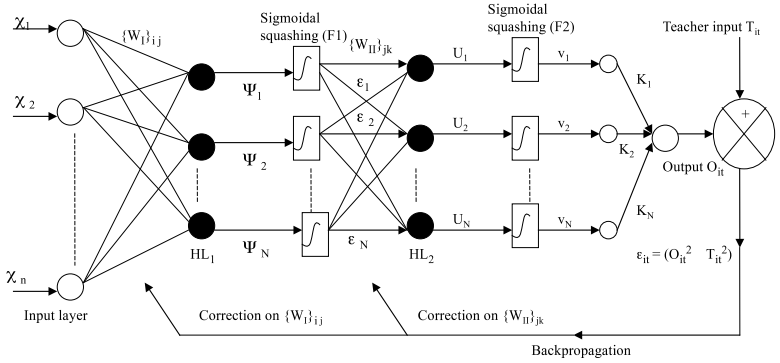

Figure 5. BPNN architecture with $\{\chi_i,\ i = 1, 2, 3, \ldots, 13\}$ depicting the feature vectors (specified in Haralick parameters deduced via GLCM) of the test image applied to input neurons of the BPNN. Teacher value corresponds to the age of the subject whose brain image is being analyzed via input data. HL_1 and HL_2 are hidden layers 1 and 2, respectively. Further, F_1 and F_2 denote sigmoidal squashing functions.

The conceived BPNN is to cohesively address and train the network with all available sets of Haralick parameters as the input and correlate them to the age of the subject. Since it is a straightforward set of input to a single output decision, the BPNN strategy is pursued.

Considering the BPNN with the entities as shown in Figure 5, its function as a backpropagation network in the training (learning) and prediction phases is summarized as follows.

Training/learning phase: This addresses the BPNN with the test image data statistics as input vectors pertinent to a subgroup of subjects whose ages are already known (and used as teacher values). That is, for each test image used in this phase, the input corresponds to the TS expressed in terms of GLCM-based Haralick parameters; and, for each input dataset (TS), the resulting net output is compared with the corresponding (known) teacher value. The computed error is then iteratively fed back to appropriately change the interconnecting weight vectors between the layers until the (mean-square) error observed at

https://doi.org/10.25088/ComplexSystems.20.4.305

the output is minimized or is less than a preset stop criterion [15, 16], such as 0.001. The sequence of functions (in Figure 5) of BPNN computations corresponds to the standard routines of a typical BPNN [14].

The TS presented to the network input layer propagates from layer to layer until the output neuron indicates an output value. If this output value is different from the desired (teacher) value, a mean-squared error is calculated and back-propagated through network layers. The weights of the interconnections are then modified proportional to the gradient of the error. Initial settings of the weights are taken as random numbers (0 to 1) of uniform distribution. In summary, the network is trained to recognize the various datasets obtained from different samples supervised by corresponding preset teacher values on age at the output. Depending on the error (depicting the difference between output and teacher value), the network weights are updated as per the resilient, gradient-descent backpropagation algorithm. Furthermore, traditional sigmoidal transfer functions of hyperbolic tangent are used between the first and second hidden layers, which enable "squashing" of layer outputs toward convergence. Also, a linear function is used between the second hidden and output layers to set appropriate scaling on the output depicting the age levels involved.

In terms of the notations indicated in Figure 5, the following are the explicit computations involved.

$$\text{Output of HL}_1 \qquad \varepsilon_j = \Psi_j \times F_1(\Psi_j), \tag{1(a)}$$

where F_1 depicts sigmoidal nonlinearity and

$$\Psi_i = \left(\sum_i (W_I)_{ij} \times \chi_i \right) + \theta_i; \qquad \theta_i \text{ is the bias/momentum.} \tag{1(b)}$$

$$\text{Output of HL}_2 = \nu_k = U_k \times F_2(U_k), \tag{1(c)}$$

where F_2 again depicts sigmoidal nonlinearity and

$$U_k = \left(\sum_j (W_{II})_{jk} \times \varepsilon_j \right) + \phi_j; \qquad \phi_j \text{ is the bias/momentum.} \tag{1(d)}$$

$$\text{Network output } O_{\text{it}} \text{ (per iteration)} = \sum_k k_k \nu_k; \tag{1(e)}$$

k_k : a linear constant

$$\text{Correction on } \{W_{II}\} j_k \; : \; \{W_{II}\} j_{k\text{-new}} = \{W_{II}\} j_{k\text{-old}} \pm (\delta \varepsilon_i / \delta \text{O}_i) \times L_1 \tag{2(a)}$$

https://doi.org/10.25088/ComplexSystems.20.4.305

$$\text{Correction on } \{W_I\}_{ij} : \{W_I\}_{ij\text{-new}} = \{W_{II}\}_{ij\text{-old}} \pm \left(\delta^2 \varepsilon_i \,/\, \delta \mathrm{O}_i^2\right) \times L_2 \qquad 2(\text{b})$$

where L_1 and L_2 are learning coefficients.

Prediction phase: Having trained the BPNN with a set of image texture details so as to indicate an output classifying the age of the subject of each test image used, the next phase is to use the BPNN in the prediction phase. That is, given image-texture data of a subject whose age is not already known and addressed at the trained BPNN input, the classifier will deliver an output prediction of the age of the subject classified into one of the values corresponding to the key images stored in the net during the training phase.

Input vector datasets: As indicated in Section 5 of this paper, the BPNN inputs correspond to the vector set of textural image features corresponding to the GLCM approach envisaged in the present study. Following the details of Haralick et al. [11], the textural feature map of the image is specified as a matrix of 13 Haralick parameters deduced from the GLCM of the image.

In the training phase, only a select subset of four Haralick parameter features are used as the TS to the network. That is, in the BPNN simulations carried out, the network reads four feature values (out of 13). Hence, the image data collected from 60 clinical volunteers/subjects and used as input vector sets correspond to a matrix of size 4×60; the corresponding supervisory (teacher) vector of 60×1 depicts the age of the subjects.

In the prediction phase, any arbitrary set of four Haralick parameters (out of 13) is considered. This select set of Haralick parameters is henceforth referred to as the prediction set (PS). Now, given a PS corresponding to a test image of a subject (with no prior information on his/her age) as the input to the trained network, it is classified compared with the stored key patterns, and the corresponding age of the subject is predicted as the output. For validation and assessing the efficacy of BPNN simulation, this predicted age is compared against the value if known clinically.

7. Experiments, Simulations, and Results

Relevant to the present study, brain image data compilation (pertinent to a subgroup of adult subjects) is done via MRI acquisitions performed on a GE 3Tesla Signa HDX system equipped with an 8-channel brain array coil. The equipment computer does Fourier transforms of the image data using a diffusion tensor imaging system. Details on the acquisition protocol are: image field-of-view (FoV) is 240×240 mm; pixel matrix size is 256×256; TR is 7400; number of diffusion direction is 25; b value is 1000; voxel size is

https://doi.org/10.25088/ComplexSystems.20.4.305

0.9375 mm × 0.9375 mm × 5 mm; slice thickness is 5 mm; and scanning time is 8 minutes. Scanning is done in the axial plane parallel to the long axis of the body of the corpus callosum. They are segmented for white matter alone.

Ten images in a specified age group, totaling 60 images of assorted male and female adult subjects without neuropathological conditions, are collected. The mean age of the subjects is 64.4483 with a standard deviation equal to 8.7841.

The BPNN simulation and image analysis are implemented in MATLAB (Version 7.6). Selecting a limited set of four inputs (as TS or PS) allows 715 possible combinations. There are 13 Haralick parameters available on each scanned image. Out of these 13, we tried to train the network with only a four input sample set without any preference. That is, as indicated in Table 1, any four parameters permutatively taken are used. There are 715 combinations of taking four out of 13. However, in order to look for the efficacy of the system, only 11 out of the 715 combinations (Table 1) were arbitrarily chosen in training the network. The network is trained with this ensemble of 11 sets. That is, with four inputs (TS) at a time in the training/learning phase, these 11 ensemble sets of TS are used to get the key vectors being stored in the constructed network. Convergence is seen in the learning phase with all training sets of the ensemble used. For example, two samples of learning curves obtained are shown in Figures 6(a) and 6(b). Mostly, the network converges between 60 and 220 iterations.

Input Sample Sets	Prediction Accuracy (%)	Input Sample Sets	Prediction Accuracy (%)
2, 3, 4, 5	94.1320	8, 9, 13, 10	90.028
1, 2, 4, 5	91.6239	8, 9, 4, 5	89.267
1, 4, 5, 6	93.1059	8, 9, 10, 12	94.341
1, 5, 6, 7	93.6209	9, 10, 11, 12	90.322
1, 6, 7, 13	89.5470		
7, 11, 10, 3	92.2900		

Table 1. Results obtained on age prediction accuracy with four input feature sets taken out of 13 GLCM-based Haralick parameters (listed in Section 4).

In the prediction phase, any arbitrary set of four inputs (out of 11 ensembles) is considered as PS and given as input to the trained network. The BPNN compares this input vector set (PS) against the stored key patterns. Hence, the classified age prediction is indicated as the output, which can be compared against the age, if already known clinically. Relevant results on prediction accuracy are presented in Table 1.

https://doi.org/10.25088/ComplexSystems.20.4.305

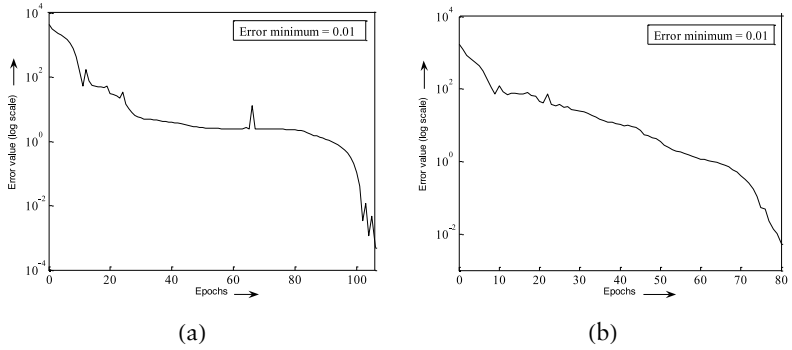

Figure 6. Sample BPNN training curves obtained with arbitrary sets of four inputs.

In addition to the testing and predictions with ensembles of four inputs, the network is expanded to include all 13 inputs as TS and/or PS. (The other architecture of the BPNN is kept unaltered.) Again, the network is seen converging around 150 epochs (Figure 7). Also in the prediction phase, the age is classified by the network accurately 96% of the time.

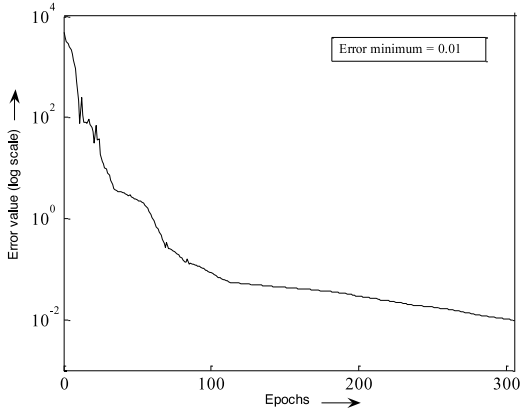

Figure 7. BPNN training curve obtained with 13 inputs.

Instead of using the GLCM-based input vectors (of Haralick parameters) gathered from the images, another set of simulation experiments is carried out with four simple statistical measures. These refer to the mean, the standard deviation, the Shannon entropy, and the variance of the normalized gray-level values [17, 18] in the 2D pixel matrix. These measures are not as extensive in describing the underlying statistics as the Haralick parameters, yet they are simpler in for-

https://doi.org/10.25088/ComplexSystems.20.4.305

mat for feature representation. When adopted in the simulations, relevant TS and PS (in lieu of GLCM features) also show convergence around 120 epochs (Figure 8) with accuracy on age prediction being about 90%.

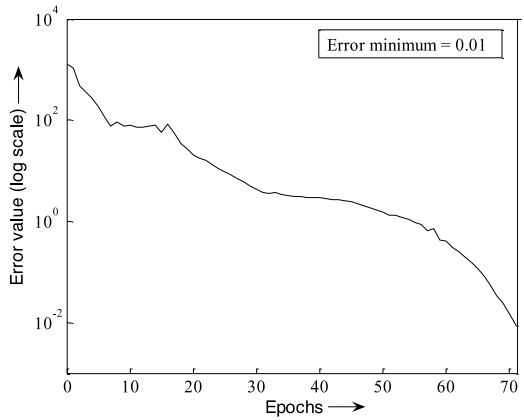

Figure 8. BPNN training curve obtained with four inputs of first order statistic measures.

Shown in Figures 9(a) through 9(d) are curves depicting various (normalized) statistical measures of the DTMRI-based Haralick parameter data versus the age of the subjects ascertained via BPNN predictions. In general, the textural features of the BWM (expressed in terms of their statistical measures) show a devolutionary trend with aging. The curve (2) in Figure 9(d), however, depicts an evolutionary trend inasmuch as it denotes a metric of information loss or entropy. Therefore, its increasing trend implicitly depicts deterioration.

8. Discussions and Conclusions

The inferential aspects of this paper are as follows.

- Prediction of age versus textural deformity of the brain complex can be done using clinical diffusion tensor magnetic resonance imaging (DTMRI) data on the brain. A backpropagation neural network (BPNN) can then be trained to classify the input of the brain's textural features and correlate such input data to the age of the subject whose brain image is analyzed.
- The clinical data collected on brain textural complexity can be organized in a statistical format of two categories:
  i. Metrics denoting relative divergence of textural features
  ii. Measures depicting the statistical features

https://doi.org/10.25088/ComplexSystems.20.4.305

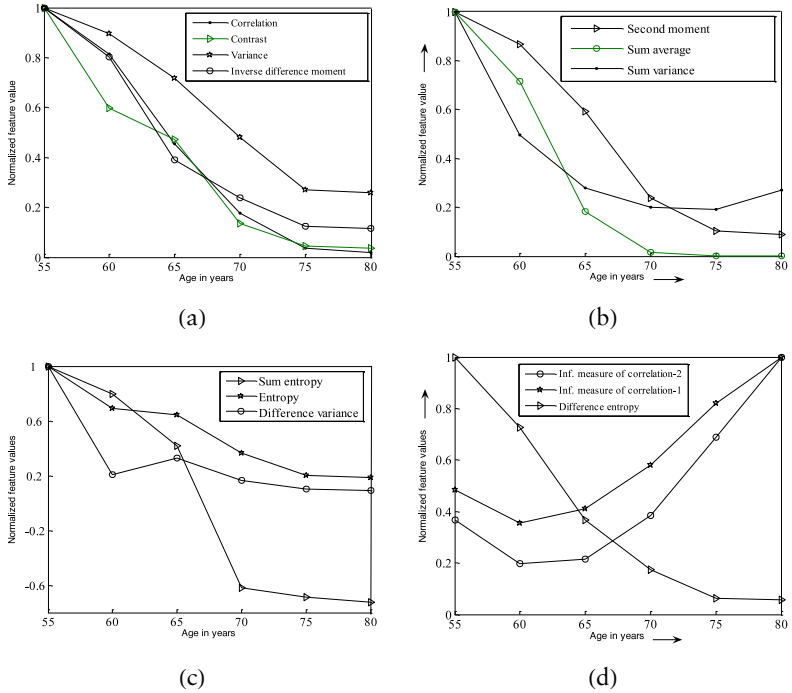

Figure 9. (a) to (d): Age versus various measures of DTMRI-based feature parameters (normalized and expressed in terms of Haralick parameter values deduced from the GLCMs of test images).

- In all, there are 13 statistical measures (known as Haralick parameters) that frame the gray level cooccurrence matrix (GLCM) of the image, which can be used for training and age prediction efforts in a classifier such as BPNN. In essence, the BPNN uses an ensemble of Haralick parameter sets as input vectors and gets trained to store corresponding feature data as key vectors. Subsequently, addressing the trained BPNN with input Haralick parameter vectors of a test image, the network classifies the input against the key vectors so as to predict the age of the subject whose brain image is tested.
- It is observed in this study that, by using only a select set of four inputs (out of 13 Haralick parameters), the BPNN shows reasonable convergence. However, the prediction accuracy is better seen when all 13 Haralick parameter inputs are exercised.
- BPNN simulation is also done with four (non-GLCM/Haralick parameter) measures based on simple statistical metrics like mean and entropy of normalized gray values in the pixel matrix. Such input data also allows the network to converge fast, but the prediction accuracy is somewhat lower than the case of using Haralick parameter metrics.

https://doi.org/10.25088/ComplexSystems.20.4.305

- The test results of this study with regard to statistical textural features of the brain white matter (BWM) complex show a devolutionary trend with aging (Figure 9). The exception of the evolutionary trend seen in curve (2) of Figure 9(d) depicts the result obtained with a metric of information loss or entropy. As such, its increasing trend therefore implicitly depicts deterioration.

As shown in Figure 9, the growing/decaying aspects of the trends in brain textural pattern versus age can be modeled as follows. The brain is a structure made of massively interconnected neural cellular parts that interact across the spatial domain; also, the associated neural activity depicts a temporal interaction between the cells. Furthermore, depending on the nature of such temporal activity involved and spatial proliferation of neural information, the underlying interaction could be largely stochastical and partly deterministic; changes in the associated physical organization and/or functional activity would lead to a significant change in the inherent self-organizational attributes of the system [2, 19]. With aging, the brain complex may pose distinct degenerative changes in its activity dynamics as well as in the mass and structural/textural features that are seen as a decrease in myelin density and alterations in myelin structure across the BWM. A simple model can be evolved to relate the associated degeneration observed versus time (aging). Suppose the textural features of the brain complex and the associated functional activity is specified by a function C, given by:

$$C(x, y, z; t) = C_o \times F(x, y, z) \times G(t) \tag{3}$$

where F and G depict independent spatial and temporal functions of the brain complex respectively and C_o is a scaling constant. The functional attributes of F and G in general are nonlinear [19] and therefore C can be more explicitly written in terms of the following logistic function with associated stochastical considerations [19]:

$$C(x, y, z; t) = C_o \times [1 - L_\alpha(s)] \times \left[1 - L_\beta(t)\right] \tag{4}$$

where α and β denote order functions ($1/2 \le \alpha < \infty$; $1/2 \le \beta < \infty$) of the stochastical profile of the brain complex and L is the Langevin–Bernoulli function depicting the nonlinear aspects of the logistic devolutions for the reasons described by Neelakanta et al. in [19]. Further, s denotes any spatial coordinate x, y, or z, and the Langevin–Bernoulli function is explicitly given by:

$$L_q(v)\, j = \left\{1 + \frac{1}{2q}\right\} \coth\left[\left(1 + \frac{1}{2q}\right)v\right] - \frac{1}{2q} \coth\left[\left(\frac{1}{2q}\right)v\right]. \tag{5}$$

When showing degenerative BWM versus aging, it can be regarded in general as the loss of information in the brain complex attributes. That is, the system entropy starts becoming overwhelmed as a result

https://doi.org/10.25088/ComplexSystems.20.4.305

of age-related degeneration. Hence the functional relation given by equation (4) is a compatible model to depict such a scenario as described in [19]. Rigorous modeling of the aforesaid nonlinear evolutions/changes in brain-textural complexity versus age needs further study.

In summary, this study enables assessing the geriatric state of a human adult subject via DTMRI images of the brain. For this purpose, the image textural data of the subject's brain is specified in statistical entities, and is used as feature vectors in an artificial neural network for training and prediction purposes. The BPNN classifies any given feature vector of the images to predict the age of the subject of the image. The test results obtained on a subgroup of adult subjects indicate, in general, a degenerative textural feature trend versus aging. Such trends can be modeled via nonlinear growth/decay considerations. Further, this work can be extended with fuzzy parameters of texture descriptions inasmuch as the gray level variations between different tissues are not abrupt. Gradual changes in gray level depict rather the nature of variations across tissues being fuzzy. Relevant fuzzy details can also be accommodated in a BPNN simulation, which forms an open question for future research.

Acknowledgment

We would like to thank Dr. R. Emmanuel, managing director of Bharat Scans Private Limited, Chennai, India, for his continuous support and guidance, and for providing necessary data throughout this research work.

References

[1] S. Wolfram, *A New Kind of Science*, Champaign, IL: Wolfram Media, Inc., 2002.

[2] A. E. Ferdinand, "A Theory of System Complexity," *International Journal of General Systems*, **1**(1), 1974 pp. 19–33.

[3] M. Ota, T. Obata, Y. Akine, H. Ito, H. Ikehira, T. Asada, and T. Suhara, "Age-Related Degeneration of Corpus Callosum Measured with Diffusion Tensor Imaging," *NeuroImage,* **31**(4), 2006 pp. 1445–1452. doi:10.1016/j.neuroimage.2006.02.008.

[4] A. Sandu, I. Rasmussen, A. Lundervold, et al., "Fractal Dimension Analysis of MR Images Reveals Grey Matter Structure Irregularities in Schizophrenia," *Computerized Medical Imaging and Graphics*, **32**(2), 2008 pp. 150–158.

[5] J. H. Silverstein, G. A. Rooke, J. G. Reves, and C. H. McLeskey, eds., *Geriatric Anesthesiology*, 2nd ed., New York: Springer, 2008.

https://doi.org/10.25088/ComplexSystems.20.4.305

[6] A. Spilt, T. Geeraedts, A. J. de Craen, et al., "Age-Related Changes in Normal-Appearing Brain Tissue and White Matter Hyperintensities: More of the Same or Something Else?," *Americal Journal of Neuroradiology*, **26**, 2005 pp. 725–729. http://www.ajnr.org/content/26/4/725.full.

[7] V. Kovalev and F. Kruggel, "Texture Anisotropy of the Brain's White Matter as Revealed by Anatomical MRI," *IEEE Transactions on Medical Imaging*, **26**(5), 2007 pp. 678–685. doi:10.1109/TMI.2007.895481.

[8] D. Tschumperle and R. Deriche, "Variational Frameworks for DT-MRI Estimation, Regularization and Visualization," in *Proceedings of the Ninth IEEE International Conference on Computer Vision (ICCV03)*, Vol. 1, Nice, France, New York: IEEE, 2003 pp. 116–121. doi:10.1109/ICCV.2003.1238323.

[9] M. Sonka, V. Hlavac, and R. Boyle, *Image Processing, Analysis, and Machine Vision*, 2nd ed., Pacific Grove, CA: PWS Publishing, 1999.

[10] J. Gorodkin, A. Sørensen, and O. Winther, "Neural Networks and Cellular Automata Complexity," *Complex Systems*, **7**(1), 1993 pp. 1–23. http://www.complex-systems.com/pdf/07-1-1.pdf.

[11] R. M. Haralick, K. Shanmugan, and I. Dinstein, "Textural Features for Image Classification," *IEEE Transactions on Systems, Man and Cybernetics*, **3**(6), 1973 pp. 610–621. doi:10.1109/TSMC.1973.4309314.

[12] J. J. Caban, A. Joshi, and P. Rheingans, "Texture-Based Feature Tracking for Effective Time-Varying Data Visualization," *IEEE Transactions on Visualization and Computer Graphics*, **13**(6), 2007 pp. 1472–1479. doi:10.1109/TVCG.2007.70599.

[13] P. A. Freeborough and N. C. Fox, "MR Image Texture Analysis Applied to the Diagnosis and Tracking of Alzheimer's Disease," *IEEE Transactions on Medical Imaging*, **17**(3), 1998 pp. 475–478. doi:10.1109/42.712137.

[14] S. Haykin, *Neural Networks and Learning Machines*, 3rd ed., New York: Prentice Hall, 2009.

[15] I. Jung and G.-N. Wang, "Pattern Classification of Back-Propagation Algorithm Using Exclusive Connecting Network," *International Journal of Computer Science and Engineering*, **2**, 2008 pp. 76–80.

[16] T. P. Vogl, J. K. Mangis, A. K. Rigler, et al., "Accelerating the Convergence of the Backpropagation Method," *Biological Cybermetics*, **59**(4–5), 1988 pp. 257–263. doi:10.1007/BF00332914.

[17] N. Sharma, A. K. Ray, S. Sharma, et al., "Segmentation and Classification of Medical Images Using Texture-Primitive Features: Application of BAM-Type Artificial Neural Network," *Journal of Medical Physics*, **33**(3), 2008 pp. 119–126. doi:10.4103/0971-6203.42763.

[18] F. Tomita and S. Tsuji, *Computer Analysis of Visual Textures*, Boston: Kluwer Academic Publishers, 1990.

[19] P. S. Neelakanta, *Information-Theoretic Aspects of Neural Network*, Boca Raton, FL: CRC Press, 1999.

https://doi.org/10.25088/ComplexSystems.20.4.305